Power Electronics Implementation of Dynamic Thermal Inertia to Offset Stochastic Solar Resources in Low-Energy Buildings

Yue Cao, *Student Member, IEEE*, John A. Magerko III, *Student Member, IEEE*, Thomas Navidi, *Student Member, IEEE*, and Philip T. Krein, *Fellow, IEEE*

***Abstract*— This paper studies the use of power electronic drives to implement dynamic thermal inertia control in low-energy buildings. Dynamic management of energy components is used to offset the variability of stochastic solar resources. Emphasis is on power electronic heating, ventilation, and air-conditioning (HVAC) drives that can act as an effective electric swing bus to mitigate the solar power variability. In doing so, grid power flows become substantially more constant, reducing the need for fast grid resources or dedicated energy storage such as batteries. The concept is equivalent to using the building thermal energy as a virtual dynamic storage in support of power grid operation. This paper defines a bandwidth over which such HVAC drives can operate. To test the methods, 18 months of solar data have been collected on submillisecond timescales as a basis to evaluate the efficacy, determine the solar frequency-domain content, and analyze the mitigation of variability. A practical bandpass filter is realized with a lower frequency bound such that the building maintains a consistent temperature, and an upper frequency bound to ensure that the commanded HVAC fan speeds do not update arbitrarily fast, avoid acoustic discomfort to occupants, and prevent undue hardware wear and tear. The combination is illustrated in simulation and with experimental results based on various update rates of a variable frequency fan drive over the stochastic solar data. Building electrical and thermal energy systems modeling is addressed, including solar and HVAC systems as well as batteries and large-scale thermal storages. A full-scale multiple-day case study provides insight into potential grid-side and storage-related benefits.**

***Index Terms*— Complex system energy management, energy-efficient buildings, grid-level energy storage, heating, ventilation, and air-conditioning (HVAC) systems, power electronic drives, solar energy, stochastic energy resources, thermal storage.**

I. Introduction

ENERGY-EFFICIENT buildings, including several net-zero energy commercial buildings, have been constructed worldwide. Research activities on this topic have increased in recent years [1]–[4], and many occupants seek net-zero energy buildings as their future offices such as the new Apple "Spaceship" in Cupertino, California [Fig. 1(a)] [5]. The Department of Electrical and Computer Engineering (ECE) at the University of Illinois–Urbana-Champaign currently occupies a 236 000 ft^2 or 22 000 m^2 facility that is targeted to become the second largest net-zero energy building in the U.S. [Fig. 1(b)] [6]. The largest is the Research Support Facility at the National Renewable Energy Laboratory in Colorado, sized at 360 000 ft^2 or 33 500 m^2 [7], as shown in Fig. 1(c).

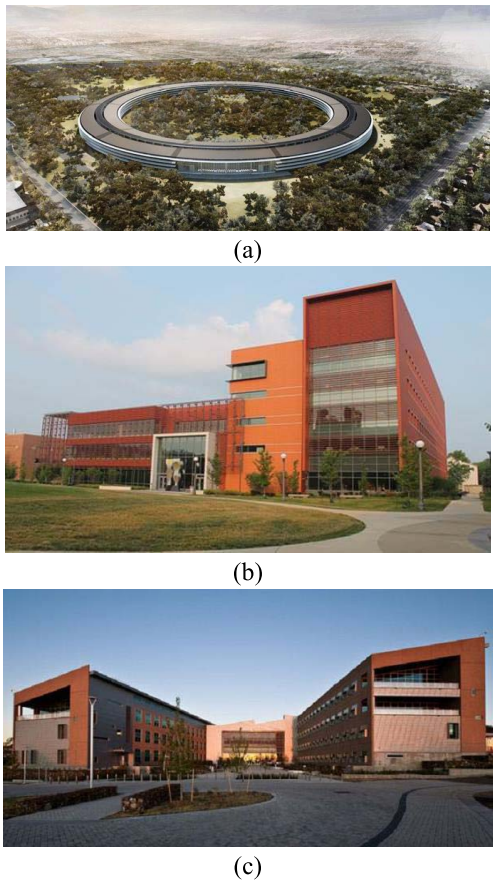

Fig. 1. Examples of large energy-efficient buildings. (a) Upcoming Apple headquarters [5]. (b) ECE building at the University of Illinois [6]. (c) Research Support Facility at the National Renewable Energy Laboratory [7].

Energy-efficient buildings, from an electrical engineering perspective, often employ onsite generated renewable energy,

Manuscript received February 4, 2016; accepted August 10, 2016. Date of publication September 13, 2016; date of current version October 28, 2016. This work was supported by the Grainger Center for Electric Machinery and Electromechanics, University of Illinois at Urbana–Champaign. A preliminary version of this paper was presented at the *2015 IEEE Energy Conversion Congress and Exposition,* Montreal, Canada [19], and at the *2015 International Conference Complex Systems Engineering,* Connecticut, USA [20]. Recommended for publication by Associate Editor H. Wang.

The authors are with the Department of Electrical and Computer Engineering, University of Illinois at Urbana–Champaign, Champaign, IL 61801 USA (e-mail: yuecao2@illinois.edu; magerko1@illinois.edu; navidi2@illinois.edu; krein@illinois.edu).

Color versions of one or more of the figures in this paper are available online at http://ieeexplore.ieee.org.

Digital Object Identifier 10.1109/JESTPE.2016.2609280

such as solar power, to support a portion of the energy demand, and therefore, to reduce the power drawn from or send excess power back to the electricity grid. Net-zero energy buildings take this concept one step further. The onsite generated renewable energy is sufficient such that on average a net-zero building does not consume energy from the grid and may provide excess power to the grid [8]. The design of such buildings is a comprehensive multidisciplinary challenge for improving construction materials, lighting systems, air condition, and thermal insulation, for example, to reduce building energy consumption. In the long run, it is envisioned that low-energy buildings will become integrated systems where renewable energy generation, electric vehicle charging, and onsite energy storage function together and interact effectively with the electricity grid. Given the various energy generation and consumption devices in a building, it is vital to manage the energy flow dynamically in such complex systems.

In energy-efficient buildings with onsite photovoltaic (PV) solar panels, the panel power can vary rapidly due to weather conditions, local intermittent shading, passing clouds or flocks of birds, differential soiling, and time of day. Although the most familiar challenge is the diurnal solar cycle (imposing substantial energy storage requirements for evening and night loads), rapid dynamic changes in solar energy are more difficult to address. Considering this inconstancy to represent an unwanted noise signal from a PV system, a suitable filter could be implemented but would require storage. Batteries or supercapacitor banks, capable of filtering fast dynamic solar power, are often discussed, but their installed size and expense can be substantial [9]–[11]. Also mentioned are hot or cold water tanks. In fact, water heating accounts for about 6% of energy usage in commercial buildings [12]. However, water is better suited for energy storage intervals of minutes to hours, given its large specific heat.

On the other hand, there is thermal storage capacity or thermal inertia inherent in the air enclosed inside a building, which can potentially act as a virtual electrical storage, much like an electric swing bus [13], [14]. Such a resource could offset fast variations in the local solar power from a grid perspective while reducing the need for conventional storage. If this can be done dynamically, thermal inertia will replace the roles of inherently expensive, fast-varying, grid-side (or building-side) resources. This is nearly equivalent to placing a low-pass filter on a building's net generation and usage, mitigating grid-side assistance until changes in the load-side demand persist beyond an extended interval [15]. Given the slow thermal response of a building, it may be anticipated that timescales of a few minutes or faster can be used to advantage to offset the resource variability without a noticeable impact on the occupants.

The unit linking the desired electrical storage and the building thermal storage is the heating, ventilation, and air-conditioning (HVAC) system, which in modern buildings is a power electronic controlled variable speed ac motor-driven energy conversion system. Power electronics enables this control via dc–dc converters, inverter-based drives, and other existing hardware, as illustrated in Fig. 2.

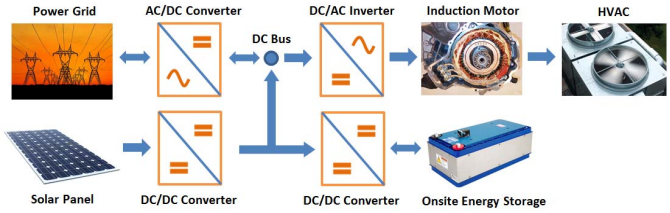

Fig. 2. Energy flow inside a building with various types of converters that may be utilized to implement dynamic energy filtering.

This paper demonstrates how intelligent control of HVAC drives can compensate, within the predetermined frequency and amplitude limits, for onsite solar power variation over short time intervals without disrupting the building temperature and comfort. The conceptual framework and methods follow from ideas in [16]–[18]. In particular, Hao *et al.* [16] and [17] show how low-pass filtering concepts can take advantage of HVAC dynamic adjustment to offset the grid-side variability, with a focus on the modest timescales associated with a power system's area control error (ACE). The results establish building thermal storage as an effective ancillary service to reduce the varying power demands from grid generators, boosting a power system's stability.

In this paper, the emphasis is on mitigating building-side dynamic variability from fast changing onsite solar generation, more akin to treating HVAC as accessing thermal inertia. Much effort is spent on determination of the full available HVAC filtering bandwidth, including lower and upper frequency bounds for slow and fast timescales associated with solar energy variations. The implementation details of the concept realization as well as the application notes with limitations will be discussed. The effectiveness of the HVAC system for mitigating the dynamic solar power changes is examined, and the potential impact on battery storage and grid regulation is evaluated (see [16], [17] for the previous results on scaling). Occupant comfort requirements, including temperature regulation and acoustic expectations, as well as fan drive hardware and software properties, limit the opportunities to adjust the HVAC operation. These previously unexplored areas will be uncovered by means of simulation and experimental data.

This paper extends prior conference presentations [19], [20] to show and test how the dynamic virtual storage concept can be implemented. The analysis here is on greater depth, and extended experimental results along with a case study are presented. Should this HVAC system-based solar power filtering concept be successfully implemented, the scaling potential would be sizeable, given that nearly 40% of the annual U.S. energy is consumed in residential and commercial buildings with nearly half of that energy consumed by HVAC systems [21], [22]. This proposed dynamic energy system management is summarized in Fig. 3. The various storage devices operate on different timescales relative to stochastic solar resources.

II. HVAC Filtering Concept Formulation

The filtering potential of thermal inertia follows from the fact that a solar power conversion system delivers output that

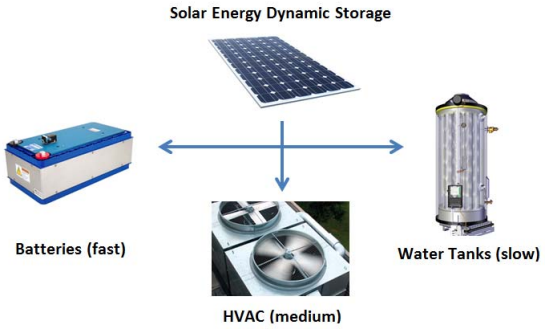

Fig. 3. Electric-thermal dynamic storage units in response to stochastic solar resources in energy-efficient buildings.

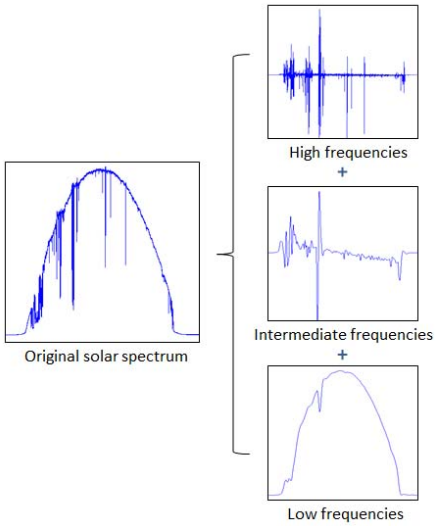

Fig. 4. Fast, medium, and slow frequency content of a typical day's solar profile (shown in a 12-h window).

contains a wide range of frequencies (more easily interpreted as timescales), ranging from a few hertz and fractions of hertz (subseconds to seconds), to multiple millihertz (minutes), and to fractions of millihertz (hours). These relatively fast, medium, and slow frequency bands are illustrated in Fig. 4, based on the measured solar power tracked during a sample day. Frequency domain analysis is therefore performed to illustrate the dynamic energy filtering concept. This analysis takes advantage of 18-month data collected from solar panels and recorded at sample rates up to 5 kHz [23].

It is important to recognize that HVAC-implemented energy resource filtering has both upper and lower frequency band limits. A lower frequency limit, meaning the lowest useful update rate for the HVAC speed and power commands, is established to shield building users from substantial temperature swings, ideally keeping variations imperceptible. An upper frequency limit, meaning the highest useful update rate for the HVAC speed and power commands, is needed such that the following conditions are met: 1) HVAC drives must be capable of responding; 2) undue wear and tear is not imposed on the drives or mechanical parts; and 3) update rates avoid discomforting audible pitch or amplitude changes. Both the

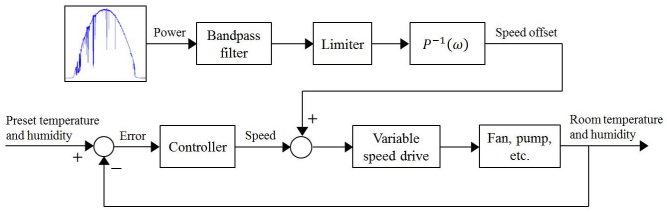

Fig. 5. Block diagrams of HVAC adjustment for dynamic thermal storage.

bounds may also be associated with amplitude limits, as rapid bang–bang control action is likely to violate conditions that determine the upper frequency bound. The approximate upper and lower frequency bounds are discussed in the subsequent sections.

If the HVAC system can effectively filter power usage over a useful frequency band, the power grid would then be better able to provide and absorb slower changes to balance the longer term building energy flow. Beyond the upper frequency boundary, more conventional onsite energy storage, such as batteries, could be used to balance the remainder. Larger scale thermal storage units such as water tanks or swimming pools [24] could be used to absorb the excess solar energy when HVAC starts to violate thermal comfort, i.e., beneath the lower frequency boundary. As a result, the power grid benefits from a slower variation in the energy demand at the building coupling point, and the conventional energy storage size is substantially reduced.

A fundamental advantage of the HVAC adjustment for effective dynamic thermal storage is that it is relatively easy to implement. It can be achieved by the fan speed-based power alteration. Conventional building energy management systems and thermostats are designed to perform in slow control loops, on timescales of minutes. The HVAC adjustment can use timescale separation and stay away from this "effective dc" loop action. In this sense, a compensation feedforward signal with zero dc content is injected into a drive to adjust the power flow on fast timescales, while avoiding interference on slow timescales. The average performance of the HVAC system remains intact, and the fast adjustment is transparent to users. Fig. 5 shows this implementation control. Bandpass filtered solar power must be applied with band and amplitude limitations before getting converted into feedforward speed offset signals via a predetermined motor speed–power relationship. The following sections explain the control loop in detail and explore the limitations. A case study using realistic parameters and data demonstrates the practicality of HVAC-based stochastic solar power filtering.

III. HVAC Filtering Lower Frequency Bound

A full 18 months of continuous data were collected from roof-mounted solar panels on the Illinois ECE department's building during 2012–13. The solar data, at 200 μs (5 kHz) intervals, are used to determine the energy-source-side bandwidth boundaries for an HVAC fan drive to support dynamic energy filtering services. Details of the data are described in [25], but the 5-kHz rate was selected to be fast enough

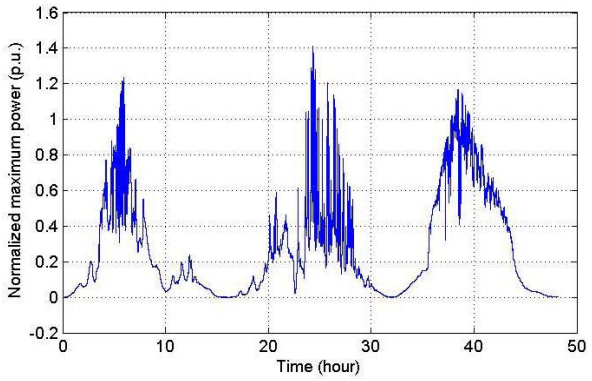

Fig. 6. Solar power profile from three sampled days (4 A.M.–8 P.M. per day).

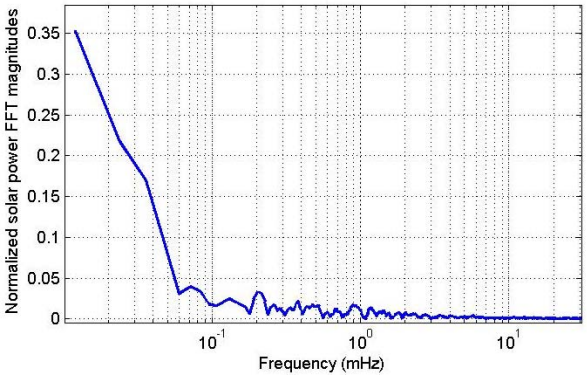

Fig. 7. Day 1 solar power profile in frequency domain (log scale).

to capture the PV power dynamics. In [23], the data show that there is minimal energy delivered by PV systems in variations faster than a few tens of hertz. Hence, extracted 50-Hz data were used for analysis in this paper.

Representative segments in the 18-month set were identified to establish the target bandwidths and the operating dynamics. For this paper, 100 days were selected at random and analyzed. A sample from three consecutive days in summer 2013 is used here to illustrate the concept. Fig. 6 shows the normalized maximum solar power per unit for this subset. Data were collected from 4 A.M. to 8 P.M. (16 h) each day to capture all sunlight. A frequency-domain analysis is shown as a semilog plot in Fig. 7. The lowest frequency components correspond to diurnal solar power changes, which essentially form a "parabola" shape of the daily solar profiles. Higher frequency components arise from dynamic cloud cover and similar changes. In particular, from Fig. 7, frequencies lower than 1 mHz (∼15 min) are associated with substantial Fourier transform (FT) magnitudes. FT magnitudes in the ∼1–20 mHz frequency range (∼15–1 min) are likely to be suitable for dynamic regulation with the building's thermal storage and HVAC system, since the internal environmental changes at this timescale are not likely to be perceptible. Note that the FT magnitudes in this range are 0.1%–1%. Frequency components above about 20 mHz are nearly absent, so update rates faster than about 30 s may be unnecessary.

With the frequency-domain analysis, the effects of an idealized HVAC system that offsets variations are modeled by

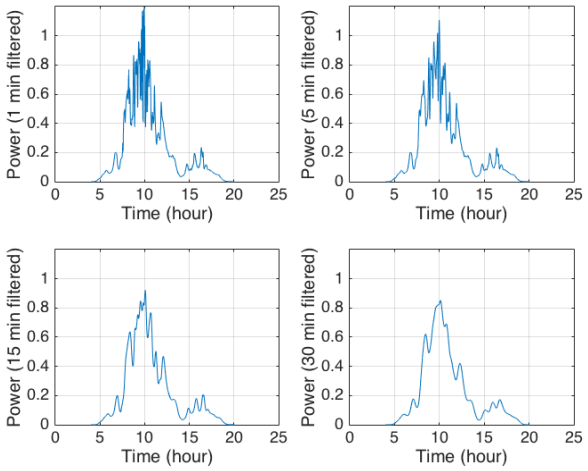

Fig. 8. Solar power profile seen from the grid after HVAC filtering effect.

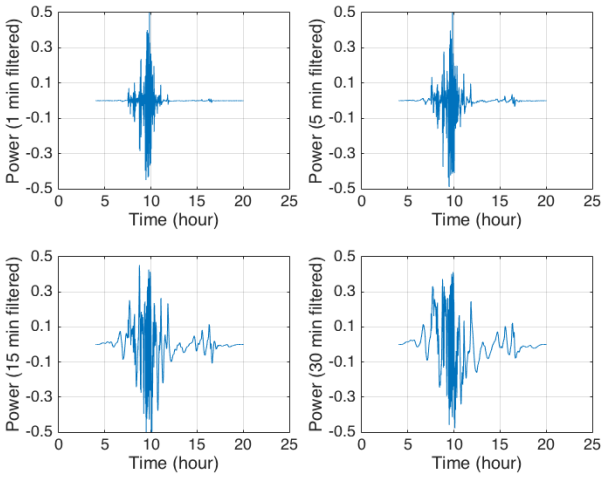

Fig. 9. Solar power to be filtered by the HVAC systems.

passing the solar data through various low-pass filters, each with a different cutoff frequency. In reality, this means that solar energy variation faster than a defined frequency limit in effect is filtered by the HVAC system without being imposed on the power grid. In other words, dynamic filtering stores or releases the building thermal energy via the HVAC system so that the grid sees a smoother net energy resource, i.e., the low-pass filtered solar waveform. Consider Day 1 from Fig. 6 as an example. Fig. 8 shows the low-pass filtered solar panel power from this day under filters with 1-, 5-, 15-, and 30-min cutoff time constants normalized to the daily maximum. Comparing Figs. 6 and 8, it appears that the filtered data with 5- and 15-min cutoff intervals are of primary interest for thermal storage regulation as they effectively eliminate rapid power change. Filtered data with a 1-min cutoff interval appear nearly identical to the original waveform and therefore dynamic filtering may not effectively mitigate variation in the solar energy if performed too quickly. 30-min filtered data are likely to make building users uncomfortable owing to excessive thermal swings, as will be documented later.

Fig. 9 shows the amount of power (per unit) filtered by the HVAC system for the filter configurations in Fig. 8.

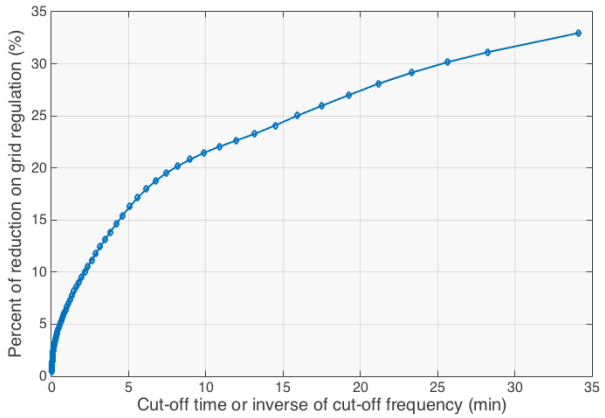

Fig. 10. Percentage of energy filtered for different cutoff intervals.

The graphs indicate the energy storage requirements, via integration, when the solar energy variation is mitigated via the building thermal energy and not by the grid. Fig. 10 summarizes the degree to which various cutoff intervals or frequencies help the grid reduce its requirements for regulation of stochastic solar energy, given that the thermal inertia is able to absorb and release this varying solar energy. The results are expressed in percentages, and shown in this way, must increase monotonically as the time interval increases. Even the 1-min cutoff interval invokes substantial energy. The band from 1 to 17 mHz (1000 to 60 s) appears to be of greatest interest for dynamic mitigation of the solar resources. The range from about a 5% (1-min buffering) to about a 25% (15-min buffering) reduction falls within this band and reduces the grid variability requirements substantially. As a result, a suitable objective is to create control mechanisms for an HVAC system that alleviates the stochastic power up to the 15-min range, or about 1 mHz. The effect is that of offsetting real, and costly, energy storage or variability resources with an essentially "free" thermal resource. One point worth emphasizing is that the processes implied by this analysis do not alter the average power or the total building energy demand from the grid, since thermal control rates faster than 1 mHz are not altered. The grid-supplied total energy required for the facility stays the same, although the grid supplies this energy more constantly rather than tracking rapid swings.

The frequency-domain analysis has determined the appropriate lower frequency bounds for the HVAC system to update the building's thermal operation based on stochastic solar resources. To demonstrate this further, the following physics-based lumped thermal model [26] of a commercial building is considered:

$$C\frac{dT(t)}{dt} = -\frac{1}{R_w}[T(t) - T_o(t)] + c_p\dot{m}(t)[T_l - T(t)] + Q_o \tag{1}$$

and the variables and constants are described in Table I [16]. This thermal model relates the air mass flow rate to the building temperature. The first term on the right-hand side of the equation represents heat loss through the walls. The second term denotes the heat gain from the HVAC system.

TABLE I
PARAMETER DESCRIPTION OF THE THERMAL MODEL

Parameter	Description	Value
C	Building thermal capacitance	7×10^5 J/°C
$T(t)$	Building room temperature	(variable) °C
R_w	Building wall thermal resistance	5×10^{-3} °C/W
$T_o(t)$	Outside air temperature	(variable) °C
$\dot{m}(t)$	HVAC air flow rate	(variable) kg/s
c_p	Air specific heat	1006 J/kg/°C
T_l	HVAC cooling air temperature	12.8 °C
Q_o	Heat gain	max 2.3×10^4 W

The third term is the heat gain from reheating, solar radiation, occupants, lighting, etc., which varies depending on the time of day. The data in Table I, originally from [16], are estimated based on measurements obtained from a 4000 m^2 university building. The outside temperature is extracted from historic data [27]. The HVAC air flow rate is determined from a linear relationship with the fan speed, whereas the fan speed follows the cube root of fan power. This fan power is linked by control with a fluctuating solar power as discussed in the previous sections. In this section, it is assumed that all of the filtered solar power in Fig. 9 is offset by the HVAC system. In summary, the following relationship holds:

$$\dot{m}(t) \propto \omega_{\text{fan}}(t) \propto P_{\text{fan}}^{1/3}(t). \tag{2}$$

In particular

$$\dot{m}(t) = k_1\omega_{\text{fan}}(t), \quad P_{\text{fan}}(t) = k_2\omega_{\text{fan}}^3(t) \tag{3}$$

where $k_1 = 0.0964$ kg/s and $k_2 = 3.3 \times 10^{-5}$ kW, and the nominal fan power is 35 kW for the sample building [16].

A MATLAB/Simulink simulation based on the thermal models and parameters is run for the four filtering scenarios in Fig. 8. The initial condition is 25 °C and a conventional HVAC system with a grid connection. Room temperature change is simulated as the stochastic solar power in Fig. 9 is offset by the building thermal mass via the HVAC system. In summer, a positive value in the solar power means additional cooling power, thus lowering the room temperature, and vice versa. As a result, four temperature profiles are simulated and presented in Fig. 11. It can be observed that there is only about a ±0.5 and ±1.5 °C change throughout the day for the 1- and 5-min cutoff filters, respectively. The ±3.0 °C change for the 15-min cutoff filter may be pushing the occupant comfort boundaries and, is likely to be noticeable, but the ±8 °C for the 30-min cutoff filter is considered too much for the occupants to accept. Although the results are unique for a given building, larger buildings with more thermal mass are likely to support 15-min filters more readily, while the large changes for the 30-min case may be almost insurmountable for conventional structures.

Summarizing the frequency-domain analysis and the thermal modeling simulation results, this paper therefore proposes that 1 mHz, the inverse of 15-min intervals, is an appropriate

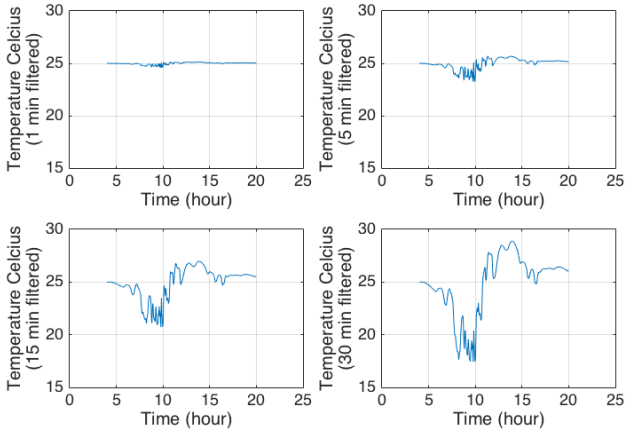

Fig. 11. Room temperature profile for different filtering scenarios.

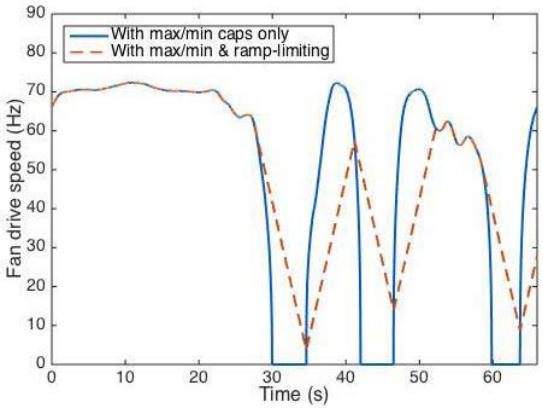

Fig. 12. Commanded speed profile with speed caps and ramp-limiting.

HVAC filtering lower frequency bound. As mentioned earlier, as many as 100 randomly selected days of solar data were analyzed and simulated, and the results support this bound. Note that the result has a similar scale with the lower cutoff frequency of 1/600 Hz, determined in [17] from a power system's ACE point of view. This bound coincides with the existing electric grid 10–15 min spinning reserve schedule [28]. Spinning reserve is the online reserve capacity synchronized to the grid and able to meet the power demand within the required time based on a dispatch instruction by an independent system operator. It is required to maintain the system frequency stability during unforeseen load swings and emergency operating conditions.

IV. HVAC Filtering Upper Frequency Bound

Hardware capabilities, including motors and drives, in addition to physical structures such as ducts and vents, determine in part the HVAC filtering upper frequency bound. To explore this, possible control schemes are set up and tested in a small HVAC system. A fan drive was characterized, and a 1/2 HP, three-phase, four-pole induction machine was coupled with a squirrel-cage fan tied to a 4-m duct, representative of typical blowers found in full-scale HVAC systems. For this experiment, the fan speed (rad/s) and the motor power (W) are related as

$$P(\omega) = 1.152 \times 10^{-5}\omega^3 + 5.205 \times 10^{-4}\omega^2 + 1.224 \times 10^{-2}\omega + 6.538 \quad (4)$$

where the coefficients were identified by a least squares fit. An initial motor drive calibration is required to produce a relationship such as (4), after which a lookup table will suffice.

There are limits on the available speeds and rates of change at any given moment, as well as acoustic constraints. In a series of tests to be described, these limitations were quantified and then used as parameters in a final version to determine the maximum feasible filtering potential that would preserve the occupant comfort and respect the drive capabilities. A three-phase 480-V Yaskawa Z1000 drive was used to control the fan speeds. This drive is in wide commercial use in HVAC systems. The drive was digitally controlled by an external computer to adjust the fan speeds with a 20-ms update rate. The high update rate permitted tracking of solar power profiles with high fidelity. In the following discussion, the fan speed is converted into electrical frequency. The baseline speed command from the drive was chosen to be 60 Hz, corresponding to the motor synchronous speed of 1800 r/min. During testing, the acoustic effects of the fan drive were recorded with a high-fidelity microphone.

There are several inherent HVAC constraints that limit the potential energy to be filtered and stored. HVAC systems have maximum and minimum power capabilities. They neither generate power nor operate above a certain power or speed limit. The maximum and minimum clamp values were required for the speed commands, within typical bounds of 0%–150%. Acoustic bounds are subjective as noticeable changes can arise from various acoustic effects. One example is fan acceleration or deceleration, in turn linked to a fan drive ramp-rate limit, in electrical hertz per second, since the rate of the motor speed changes directly influences the recurrence rate of the acoustic peaks. The ramp-rate limit was established based on acoustic data and subjective reactions.

To illustrate the audio analysis, a sample solar power profile was chosen from Day 1 in Fig. 6, spanning approximately 1 min starting at 10:00 A.M. This sample was selected because it includes a mix of relatively constant (±3%) and rapidly varying (±20%) power. The solar profile data faster than the previously determined 1 mHz lower frequency bound were filtered and fed as a feedforward offset into the HVAC system. From the experiment, a limit preventing the blower from ramping between 0% and 150% speed in less than 10 s was found to be acceptable. In other words, the suitable ramp rate limit was determined to be 9 Hz/s. This ramp rate is much slower than the maximum response rate of the drive and is therefore likely to avoid concerns about undue wear and tear. The motor/fan speed command abiding by this limitation using the 1-min solar profile is shown in Fig. 12, along with a purely capacity-limited speed command. Fig. 13 depicts audio samples measuring amplitude changes for the motor profiles without and with ramp-limiting controls, in the positive and negative parts of Fig. 13, respectively. The negative side is the inverse of the magnitudes, presented

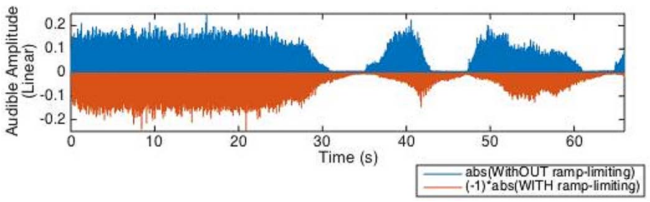

Fig. 13. Measured fan sound in amplitude for motor/fan speed commands without and with ramp-limiting. The case with ramp limits is shown as negative values to support direct comparison.

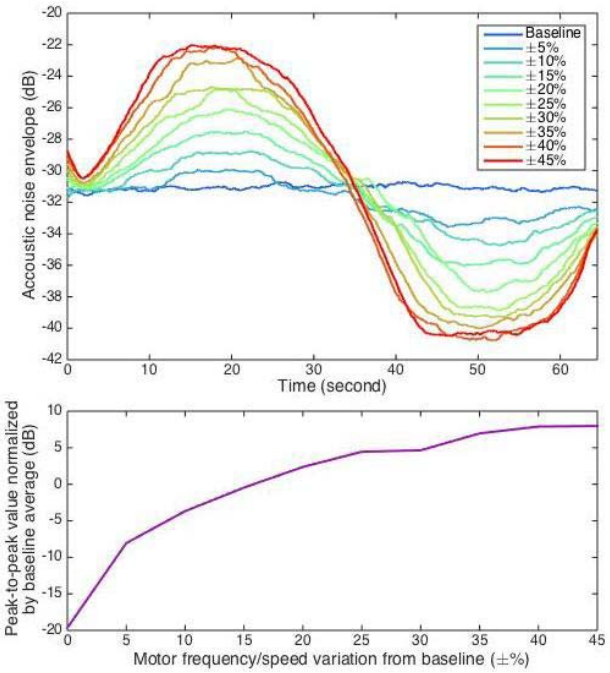

Fig. 14. Acoustic noise amplitude (top) and relative amplitude change compared with baseline (bottom) for various sinusoidal fan speed profiles.

for comparison purposes. Most noticeable in Fig. 13 are the slower and smoother amplitude changes in the ramp-limited case, which is acoustically more comfortable to the building occupants. However, reduced amplitudes and delayed responses in this case result in diminished HVAC filtering capability with respect to the stochastic solar power.

Absolute changes in the pitch or audible frequency content are inherent to speed changes and specific blower architectures. Therefore, after determining how fast the sound pitches are allowed to change, attention was given to the filtering limits imposed by how much the acoustic amplitudes may change at once. This limit avoids the excessive rise and fall in loudness from the ducts and vents. A series of acoustic tests, injecting several 1-min sinusoidal speed commands with various amplitudes into the motor drive controller, was conducted. Taking 60 Hz as the baseline speed, the speed amplitudes varied by $\pm 5\%, \pm 10\%, \ldots, \pm 45\%$, with 90 Hz as the absolute maximum speed. The respective recorded noise envelopes in dB are shown in the top half of Fig. 14. The bottom half is the peak–peak amplitude of each curve compared with the baseline magnitude to generate a normalized expectation about

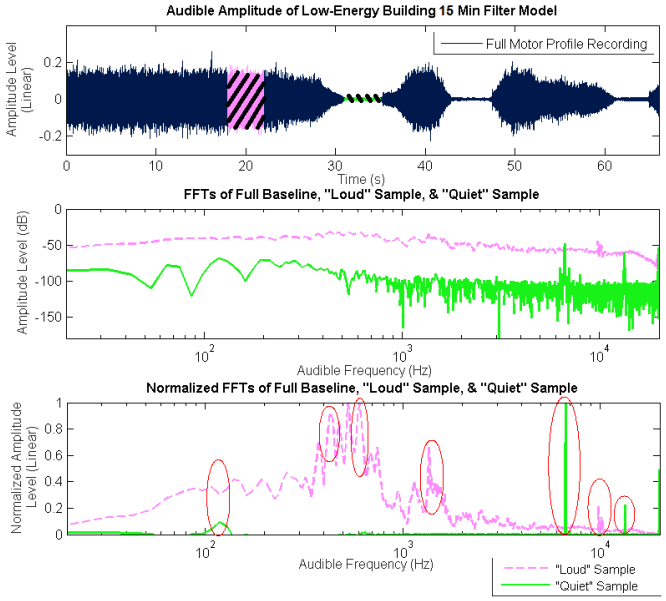

Fig. 15. Measured sound amplitudes across audible frequency spectrum for the baseline, "Loud" sample, and "Quiet" sample.

amplitude variations. A speed variation corresponding to 0 dB, or equivalently a peak-to-peak change equal to the baseline magnitude ($\pm 16\%$), was found to be imperceptible. This means that about 50 and 70 Hz are the appropriate minimum and maximum fan speed limits when the fan operates around the baseline of 60 Hz. Amplitude limits using absolute fan speed changes of ± 10 Hz are implemented across the full motor operating range.

In addition to amplitude changes, shifts in the dominant audible frequencies occur when following a filtered solar power profile. These dominant frequencies can originate from motor properties, structural resonances, or effects in the HVAC system. Fig. 15 highlights the recorded sound amplitudes, without the ramp-rate limited control, across the audible spectrum when moving from a high-speed "Loud" regime to a low-speed "Quiet" regime as designated by the left and right shaded regions in the top part of Fig. 15. The middle depicts the frequency content so that the frequency amplitudes can be compared. The bottom half of Fig. 15 normalizes the peak frequency amplitudes to isolate the pitch from changes in the amplitude. The circled regions indicate the dominant frequencies that arise or become noticeably absent relative to the baseline operation and would likely contribute to the conspicuousness of the speed changes. This analysis emphasizes the importance of the ramp-rate and amplitude limits.

After determining the speed and acoustic constraints using the scaled down HVAC fan drive, a MATLAB model was created to extrapolate to a building-level implementation. Fig. 16 depicts a 1-min sample of this power curve in gray. The HVAC filtering capabilities can be found by integrating the area under the dashed curve and under the gray region and then finding the ratio between the two. This was done by stepping through each time and determining the filtration desired and available based on the solar fluctuations,

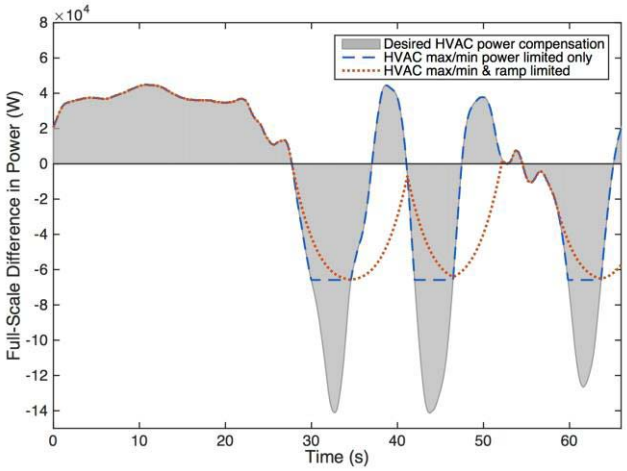

Fig. 16. Desired power compensation requested from full-scale HVAC systems with and without speed clamps and ramp limiting.

fixed capacity limitations, and dynamic acoustic limitations. The ramp-limited case is more complicated because, as observed in Fig. 16, the power consumption represented by the dotted curve cannot always be tracked and is effectively time-delayed relative to the ideal filter. Thus during periods of rapid power fluctuation, there are times during which the HVAC filter is potentially counterproductive because of acoustic-based slew limits.

Given the operating limitations and the need for long-term occupant comfort, only a fraction of the HVAC capacity in a building is available for filter implementation. In the proposed approach, the ventilation fan speed is the primary mechanism, and this in turn is a portion of the HVAC consumption. For a quick estimate, since the operating frequency range can be adjusted to $\pm 16\%$, the fact that the fan power changes as the cube of speed suggests that the ventilation power can be adjusted up to about $\pm 40\%$ on millihertz or faster timescales. For a building in which 20% of the energy consumption is for ventilation, this provides a fast $\pm 8\%$ change capability in the total building energy consumption. Simulation analysis suggests a more optimistic result, since the $\pm 16\%$ limit is not always reached depending on the weather, and when the operating frequency is below 60 Hz, the percentage limit is higher.

During simulation, when the acoustic constraints are included and the assumption of 20% ventilation energy consumption in a building is made, it is found that the HVAC filtering capability is, on average, 56.6%, 36.9%, and 17.3% for buildings with PV installations rated at 25%, 50%, and 100% of average building load, respectively, over the course of randomly selected 100 days from the solar database. Fig. 17 shows this complete trend in solid black lines. In Fig. 17(a), larger ventilation energy consumed in building loads results in a higher capability for the HVAC system to mitigate the dynamic solar power. A building's regional weather pattern also affects the HVAC filtering capability. Steady sunny days are favored, and days with fluctuating solar radiation are undesirable, as illustrated in Fig. 17(b). The general takeaway from

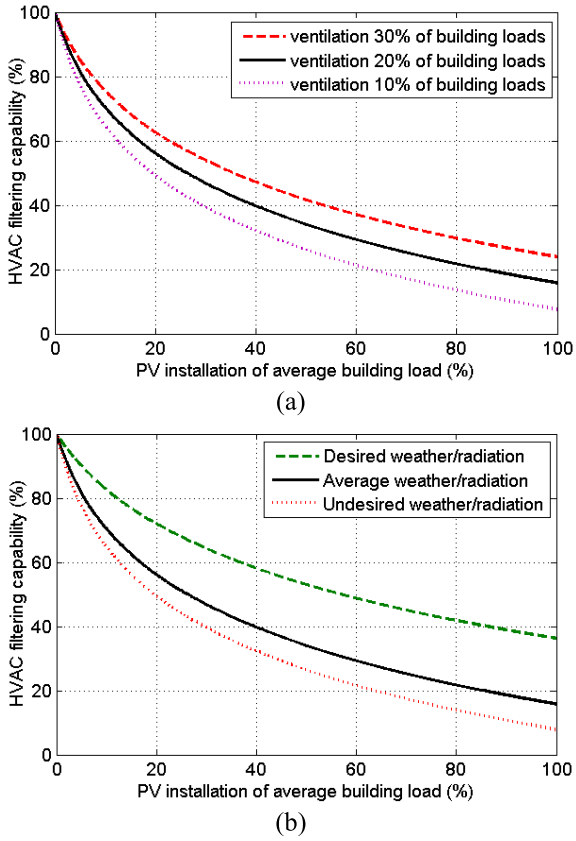

Fig. 17. HVAC filtering capability changes at various solar installation capacities based on (a) percentage of ventilation energy consumed in building and (b) various weather conditions.

this analysis is that realistic HVAC filter implementation can offset a substantial fraction of the solar variability to timescales of about 15 min, helping to bring solar resources into a more conventional utility dynamic management interval [29]. This approach is not self-sufficient for large PV installations and they must rely on additional energy storage devices or on the grid.

In summary, the fan drive and acoustic experiments suggest 0.1 Hz, or the inverse of a 10-s interval, to be a plausible upper frequency bound. The result improves on the upper cutoff frequency of 1/8 Hz in [17], which is estimated from the implicit mechanical stress and ACE sampling rate. Acoustic frequency changes and amplitude limits impose extra constraints on the control of the fan drive operation. The HVAC filtering capability is therefore reduced. However, the capability varies depending on the percentage of installed PV generation given a building's load, the percentage of HVAC loads in the building, and the solar radiation conditions.

V. Case Study Demonstration

To demonstrate and validate the potential of dynamically controlled HVAC loads that implement filtering of the stochastic energy content, a small fan drive was first used to follow scaled responses to various band-limited solar power profiles. The results were then employed in a full-scale model to determine the building-level filtering potential.

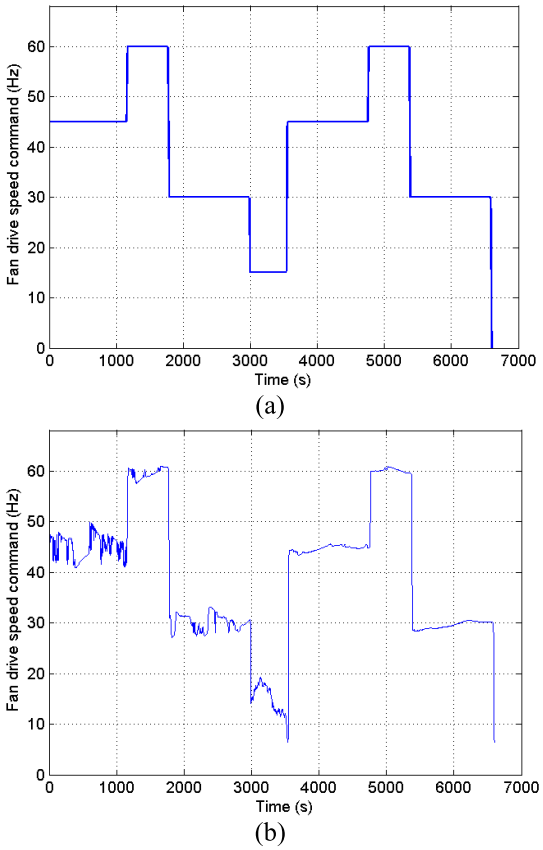

Fig. 18. Fan drive speed profile (a) without and (b) with dynamic HVAC filtering.

For direct tests, the Z1000 drive with a motor and duct was fed with two speed command profiles for approximately 2 h. The first speed profile is a piecewise constant signal to represent the conventional HVAC loop control, as shown in Fig. 18(a). From time to time the fan speed has step changes, but for the majority of the time it is held constant. The second speed profile implements a feedforward signal injected control loop as in Fig. 5. The feedforward signal is generated from bandpassed (1 mHz–0.1 Hz) solar power (10 A.M.–12 P.M. in Fig. 8) followed by speed calculation from the relationship in (4). Acoustic constraints are enforced. Fig. 18(b) shows the resulting combined speed commands. As would be expected, the speed changes are more sensitive to the power variations at lower speeds due to the cubic power–speed relationship. The experiments collected two sets of power consumed by the fan system and measured the difference, which represents the fluctuating power to be mitigated. This measured power difference along with the modeled result is plotted in Fig. 19. Except during short transients when the motor steps, the modeled curve follows the experimental curve closely, providing an accurate basis for a large-scale multiple-day simulation. Although the magnitudes in Fig. 19 appear small, they are approximately 10% of the full magnitudes during this experiment using the small fan drive.

The lower frequency bound provides an opportunity for larger scale thermal storage such as water tanks to store

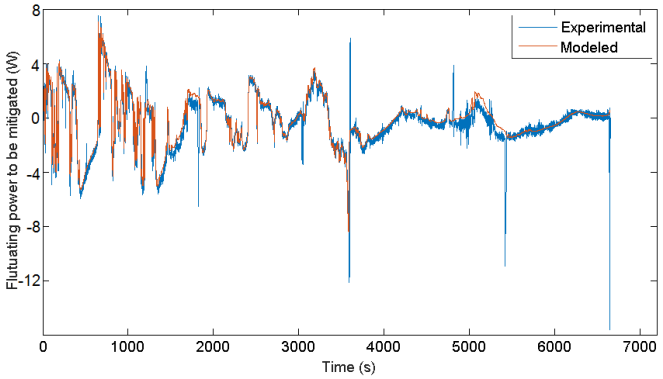

Fig. 19. Power difference consumed by the fan drive between the two speed profiles.

or compensate solar energy at slow rates, while the upper frequency bound probably requires batteries to react to fast solar radiation changes. An additional MATLAB simulation is performed when utilizing batteries, HVAC, and water tanks together as shown in Fig. 3, while imposing several days of solar profile, selecting 1 mHz and 0.1 Hz as the HVAC filtering lower and upper frequency bounds, and taking into consideration the acoustic amplitude and ramp-rate limits. This particular case study assumes an energy-efficient building with solar installation at peak 300 kW and an HVAC system at 150 kW capacity of which 20% is used by ventilation. The power grid is modeled to track the solar profile with moving average step responses every 15 min, similar to the role of the conventional spinning reserve. Ten random days out of the 18-month database were simulated for analysis; the results from one sample day as shown in Fig. 8 are illustrated in Figs. 20–22.

Fig. 20 depicts the conventional scenario in which all stochastic solar energy is supported by the grid (by means of grid-based external storage or spinning reserve). The situation in Fig. 21 is much improved with assistance from building thermal inertia alone via HVAC filtering. In Fig. 22, if water tanks are included and can effectively mitigate the solar power on scales slower than 1 mHz, the grid experiences a minimal power fluctuation except when fast solar power variations cannot be filtered due to acoustic and ramp-rate limits. A battery storage requirement can be calculated for each scenario by integrating the area under the battery power curve and finding the peak value. Over the course of these 10 days, a total of 53.0-kWh battery energy is required for grid support when filtering is not engaged. With HVAC for dynamic energy regulation, this number drops to 39.1 kWh. For the final combined scenario, only 2.68 kWh of battery capacity is necessary. Not only is the battery storage reduced, but also the amount of energy entering and exiting the battery is drastically reduced. In this particular sample day from Fig. 20, 34.80 and 120.12 kWh energy flows are eliminated for the scenarios in Figs. 21 and 22, respectively. The power electronics converter (see Fig. 2) losses as a result of these energy flows can therefore be avoided and the battery life can be improved due to less frequent energy flowing in and out.

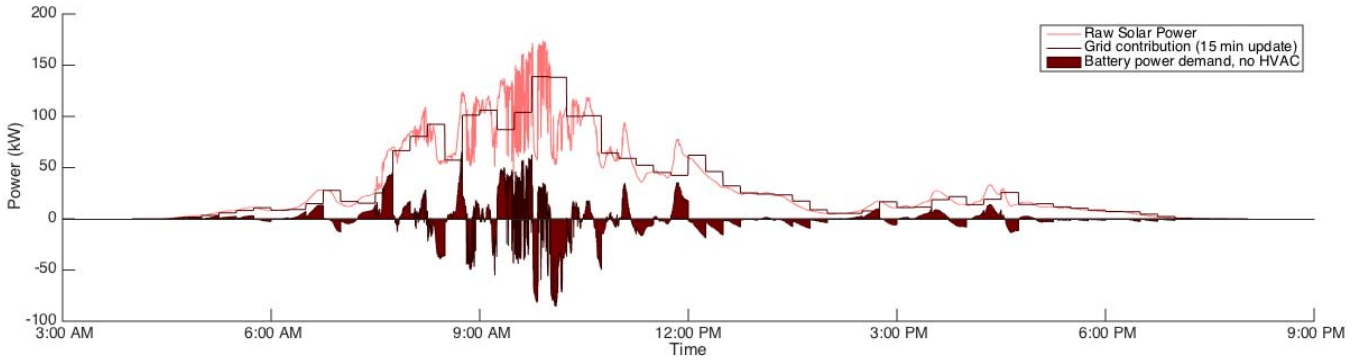

Fig. 20. Grid and battery energy contribution imposed by raw solar data.

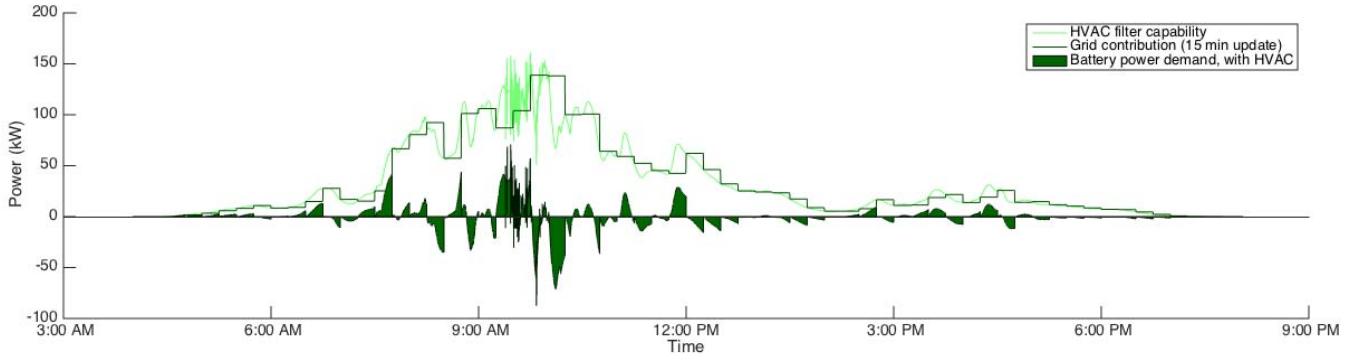

Fig. 21. Grid and battery energy contribution when proposed HVAC dynamic filtering is at work.

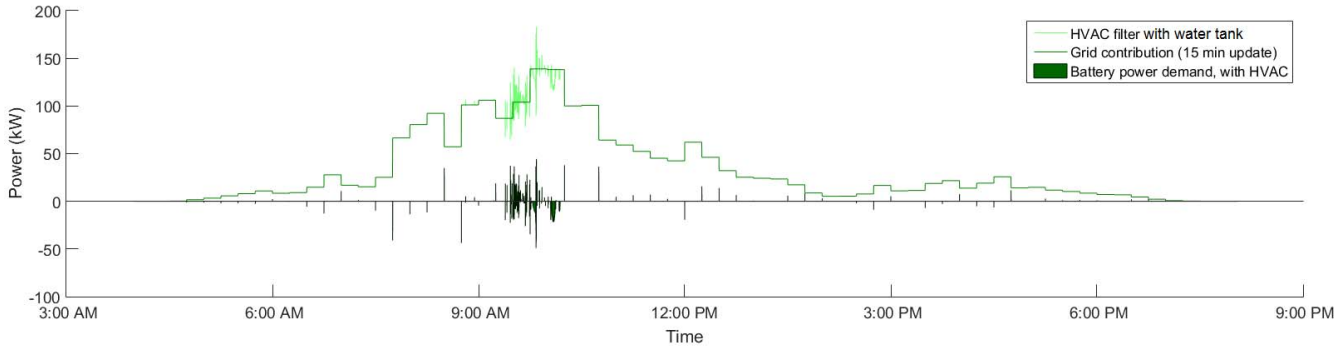

Fig. 22. Grid and battery energy contribution when both HVAC dynamic filtering and water tanks are at work.

VI. Conclusion

This paper discusses the use of power electronics to implement the dynamic thermal inertia to offset stochastic solar resources, especially in low-energy buildings. It builds on ideas introduced in [16] and [17] to set up a dynamic energy balancing and storage solution linked to HVAC systems. It focuses on dynamic mitigation of building-side rapid solar energy variations through an energy filtering concept. In a practical implementation, the lower HVAC update frequency limit is shown to be about 1 mHz (the inverse of 15 min) and limits the temperature variations in occupied spaces while reducing the conventional long-term onsite energy storage needs. The higher update frequency limit in the range of about 0.1 Hz (the inverse of 10 s), combined with ramp-rate and acoustic limits, lets a ventilation drive respond without generating annoying noise and reduces short-term onsite electrical energy storage needs, such as batteries. The process has been demonstrated based on solar data frequency-domain analysis and system-level electrical and thermal interaction modeling, as well as fan drive experiments. A full-scale multiple-day simulation case study has provided insight into the potential grid-side and storage-related benefits. This paper has discovered that the practical solar energy filtering capability of an HVAC system varies with multiple factors that include installed solar capacity, regional weather patterns, building functionality, and dynamic building usage.

Although the HVAC filtering lower and upper frequency bounds are restricted by the occupant comfort, the constraints

can be relaxed for some buildings used for unmanned environments, such as data centers or product warehouses. While a single building's thermal inertia may not be enough to mitigate the solar energy variability for its entire supply, neighboring nonsolar buildings can be retrofitted to contribute their thermal inertia to assist in the same fashion.

ACKNOWLEDGMENT

The authors would like to thank the efforts of R. C. N. Pilawa-Podgurski and his students for obtaining the long-term fast solar data.

REFERENCES

[1] X. Guan, Z. Xu, and Q.-S. Jia, "Energy-efficient buildings facilitated by microgrid," *IEEE Trans. Smart Grid*, vol. 1, no. 3, pp. 243–252, Dec. 2010.

[2] Z. Wang, R. Yang, and L. Wang, "Multi-agent control system with intelligent optimization for smart and energy-efficient buildings," in *Proc. Annu. Conf. IEEE Ind. Electron. Soc. (IECON)*, Nov. 2010, pp. 1144–1149.

[3] T. Wei *et al.*, "Battery management and application for energy-efficient buildings," in *Proc. ACM/EDAC/IEEE Design Autom. Conf.*, Jun. 2014, pp. 1–6.

[4] E. Saberbari and H. Saboori, "Net-zero energy building implementation through a grid-connected home energy management system," in *Proc. Conf. Electr. Power Distrib. Netw. (EPDC)*, May 2014, pp. 35–41.

[5] Sky News. *Apple Campus Approved by Cupertino Council*, accessed on Oct. 17, 2013. [Online]. Available: http://news.sky.com/story/1155428/apple-campus-approved-by-cupertino-council

[6] C. Sandberg, P. Krein, D. Bodenschatz, and K. Fernandes, "Energy optimization in a performance-driven culture—The new electrical and computer engineering building at the University of Illinois," presented at the Building Chicago Greening Heartland Conf., Chicago, IL, USA, Sep. 2013.

[7] DOE (U.S. Department of Energy), "Research support facility—Leadership in building performance," Nat. Renew. Energy Lab., Golden, CO, USA, Tech. Rep. DOE/GO-102011-13311, Sep. 2011.

[8] S. Pless and R. Torcellini, "Net-zero energy buildings: A classification systems based on renewable energy supply options," Nat. Renew. Energy Lab., Golden, CO, USA, Tech. Rep. NREL/TP-550-44586, Jun. 2010. [Online]. Available: http://www.nrel.gov/sustainable_nrel/pdfs/44586.pdf

[9] Z. Xu, X. Guan, Q.-S. Jia, J. Wu, D. Wang, and S. Chen, "Performance analysis and comparison on energy storage devices for smart building energy management," *IEEE Trans. Smart Grid*, vol. 3, no. 4, pp. 2136–2147, Dec. 2012.

[10] C. J. C. Williams, J. O. Binder, and T. Kelm, "Demand side management through heat pumps, thermal storage and battery storage to increase local self-consumption and grid compatibility of PV systems," in *Proc. IEEE PES Int. Conf. Innov. Smart Grid Technol.*, Oct. 2012, pp. 1–6.

[11] T. Zhou and W. Sun, "Optimization of battery–supercapacitor hybrid energy storage station in wind/solar generation system," *IEEE Trans. Sustain. Energy*, vol. 5, no. 2, pp. 408–415, Apr. 2014.

[12] (May 2009). *Buildings Overview, Center for Climate and Energy Solutions*. [Online]. Available: http://www.c2es.org/technology/overview/buildings

[13] Y. Ma, A. Kelman, A. Daly, and F. Borrelli, "Predictive control for energy efficient buildings with thermal storage: Modeling, stimulation, and experiments," *IEEE Control Syst.*, vol. 32, no. 1, pp. 44–64, Feb. 2012.

[14] C. Szasz, "HVAC elements modeling and implementation for net-zero energy building applications," in *Proc. IEEE Int. Symp. Appl. Comput. Intell. Informat. (SACI)*, May 2014, pp. 195–200.

[15] M. Maasoumy, B. M. Sanandaji, K. Poolla, and A. Sangiovanni-Vincentelli, "Model predictive control of regulation services from commercial buildings to the smart grid," in *Proc. Amer. Control Conf. (ACC)*, Jun. 2014, pp. 2226–2233.

[16] H. Hao, T. Middelkoop, P. Barooah, and S. Meyn, "How demand response from commercial buildings will provide the regulation needs of the grid," in *Proc. 50th Annu. Allerton Conf.*, Oct. 2012, pp. 1908–1913.

[17] H. Hao, Y. Lin, A. S. Kowli, P. Barooah, and S. Meyn, "Ancillary service to the grid through control of fans in commercial building HVAC systems," *IEEE Trans. Smart Grid*, vol. 5, no. 4, pp. 2066–2074, Jul. 2014.

[18] J. D. Glover and F. C. Schweppe, "Advanced load frequency control," *IEEE Trans. Power App. Syst.*, vol. PAS-91, no. 5, pp. 2095–2103, Sep. 1972.

[19] Y. Cao, J. A. Magerko, T. Navidi, and P. T. Krein, "Dynamic filtering of stochastic solar resources using HVAC drive control—A determination of feasible bandwidth," in *Proc. IEEE Energy Convers. Congr. Expo (ECCE)*, Sep. 2015, pp. 3127–3134.

[20] Y. Cao, J. A. Magerko, T. Navidi, and P. T. Krein, "Dynamic energy management needs in low-energy buildings imposed by stochastic solar resources," in *Proc. Int. Conf. Complex Syst. Eng. (ICCSE)*, Nov. 2015, pp. 1–6.

[21] P. Hernandez and P. Kenny, "From net energy to zero energy buildings: Defining life cycle zero energy buildings (LC-ZEB)," *Energy Buildings*, vol. 42, no. 6, pp. 815–821, Jun. 2010.

[22] L. Pérez-Lombard, J. Ortiz, and C. Pout, "A review on buildings energy consumption information," *Energy Buildings*, vol. 40, no. 3, pp. 394–398, 2008.

[23] J. A. Magerko, Y. Cao, and P. T. Krein, "Quantifying photovoltaic fluctuation with 5 kHz data: Implications for energy loss via maximum power point trackers," in *Proc. IEEE Power Energy Conf. Illinois (PECI)*, Feb. 2016, pp. 1–7.

[24] S. Meyn, P. Barooah, A. Busic, and J. Ehren, "Ancillary service to the grid from deferrable loads: The case for intelligent pool pumps in Florida," in *Proc. IEEE Conf. Decision Control (CDC)*, Dec. 2013, pp. 6946–6953.

[25] R. J. Serna, B. J. Pierquet, J. Santiago, and R. C. N. Pilawa-Podgurski, "Field measurements of transient effects in photovoltaic panels and its importance in the design of maximum power point trackers," in *Proc. IEEE Appl. Power Electron. Conf.*, Mar. 2013, pp. 3005–3010.

[26] A. F. Mills, *Heat Transfer*, 2nd ed. Upper Saddle River, NJ, USA: Prentice-Hall, 1998, pp. 61–105.

[27] *Weather Underground*, accessed on Jun. 20, 2015. [Online]. Available: http://www.wunderground.com/

[28] North American Electric Reliability Corporation (NERC). *Ancillary Services Matrix—Spinning Reserve*, accessed on Nov. 15, 2015. [Online]. Available: http://www.nerc.com/

[29] P. Samadi, H. Mohsenian-Rad, V. W. S. Wong, and R. Schober, "Tackling the load uncertainty challenges for energy consumption scheduling in smart grid," *IEEE Trans. Smart Grid*, vol. 4, no. 2, pp. 1007–1016, Jun. 2013.

Yue Cao (S'08) received the B.S. (Hons.) degree in electrical engineering with a second major in mathematics from the University of Tennessee, Knoxville, TN, USA, in 2011, and the M.S. degree in electrical engineering from the University of Illinois at Urbana–Champaign (UIUC), Champaign, IL, USA, in 2013, where he is currently pursuing the Ph.D. degree with the Power and Energy Systems Group.

He has been a Power Electronics Engineer Intern with Apple Inc., Cupertino, CA, USA, Halliburton Company, Houston, TX, USA, Flanders Electric, Evansville, IN, USA, and the Oak Ridge National Laboratory, Oak Ridge, TN, USA, in addition to research and teaching. His current research interests include power electronics, motor drives, and energy storage with applications in transportation electrification, renewable energy integration, and energy efficient buildings.

Mr. Cao was a recipient of the Myron Zucker Student Award from the IEEE Industry Applications Society in 2010. He is currently a Sundaram Seshu Fellow with UIUC, where he was a James M. Henderson Fellow in 2012. From 2012 to 2013, he was the President of the IEEE PES/PELS/IAS Student Chapter with UIUC. He has been rated as an Excellent Teaching Assistant for multiple years since 2013. He was the Webmaster for the 2009, 2010, and 2012 IEEE Energy Conversion Congress and Exposition. He was the Corresponding Technical Programs Chair of the 2016 IEEE Power and Energy Conference at Illinois. Since 2014, he has been an Invited Reviewer for eight different IEEE Transactions or journals and one IET journal.

John A. Magerko III (S'15) received the B.S. (Hons.) and M.S. degrees in electrical engineering from the University of Illinois at Urbana–Champaign (UIUC), Champaign, IL, USA, in 2014 and 2016, respectively. His thesis work focused on photovoltaic energy integration, energy efficient buildings, power electronics, and alternative energy storage mechanisms.

From 2012 to 2014, he was a Research Assistant with the United States Army Corps of Engineers, Construction Engineering Research Laboratory, Engineering Research and Development Center, Champaign, IL, USA. He is the listed Co-Inventor on a patent disclosure entitled *Non-Rotary, Natural Wind Based, Electrical Power Generating Method and Associated Electronic Control Circuitry for Energy Use and/or Storage*.

Mr. Magerko was a recipient of the 2016 Grainger Award from the Grainger Center for Electric Machines and Electromechanics. He was the Publicity Chair of the 2016 IEEE Power and Energy Conference at Illinois and served as the 2015-2016 Vice President of the IEEE PES/PELS/IAS Student Chapter at UIUC.

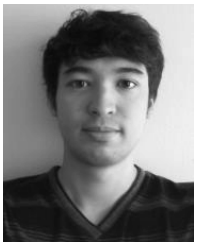

Thomas Navidi (S'15) received the B.S. degree in electrical engineering from the University of Illinois at Urbana–Champaign (UIUC), Champaign, IL, USA, in 2016. He is currently pursuing the Ph.D. degree in electrical engineering with specialization in power electronics with Stanford University, Palo Alto, CA, USA.

He was a Research Assistant with the Grainger Center for Electric Machinery and Electromechanics, UIUC. He has been a Power Engineering Intern with Bechtel Corporation, Pueblo, CO, USA.

Mr. Navidi was a recipient of the Grainger Power Engineering Award from UIUC upon graduation.

Philip T. Krein (S'76–M'82–SM'93–F'00) received the B.S. degree in electrical engineering and the B.A. degree in economics and business from Lafayette College, Easton, PA, USA, and the M.S. and Ph.D. degrees in electrical engineering from the University of Illinois at Urbana–Champaign (UIUC), Champaign, IL, USA.

He was an Engineer with Tektronix, Beaverton, OR, USA, and then returned to UIUC. From 1997 to 1998, he was a Senior Fulbright Scholar with the University of Surrey, Guildford, U.K. From 2003 to 2014, he was a Founder and a member of the Board of Directors of SolarBridge Technologies, Inc., Austin, TX, USA, a developer of long-life integrated inverters for solar energy, and currently a part of Sunpower, San Jose, CA, USA. He is currently the Grainger Endowed Chair Emeritus in Electric Machinery and Electromechanics and the Director of the Grainger Center for Electric Machinery and Electromechanics with UIUC. He is also the Executive Dean of the Zhejiang University-UIUC Institute for Engineering, Haining, China. He holds 34 U.S. patents with additional patents pending. His current research interests include power electronics, machines, drives, electric transportation, and electrical energy, with an emphasis on nonlinear control approaches.

Dr. Krein was a recipient of the IEEE William E. Newell Award in Power Electronics in 2003. He has served as the President of the IEEE Power Electronics Society and a member of the IEEE Board of Directors. He is a Registered Professional Engineer at Illinois and Oregon. From 2015 to 2016, he is the Chair of the IEEE Transportation Electrification Community. He was elected to the U.S. National Academy of Engineering in 2016. In 2001, he helped to initiate the International Future Energy Challenge, a major student competition involving fuel cell power conversion and energy efficiency. He is the Editor-at-Large of the IEEE TRANSACTIONS ON POWER ELECTRONICS and an Associate Editor of the IEEE JOURNAL OF EMERGING AND SELECTED TOPICS IN POWER ELECTRONICS.